A Middle Eocene lowland humid subtropical "Shangri-La" ecosystem in central Tibet

Tao Su[a,b,c,1], Robert A. Spicer[a,d], Fei-Xiang Wu[e,f], Alexander Farnsworth[g], Jian Huang[a,b], Cédric Del Rio[a], Tao Deng[c,e,f], Lin Ding[h,i], Wei-Yu-Dong Deng[a,c], Yong-Jiang Huang[j], Alice Hughes[k], Lin-Bo Jia[j], Jian-Hua Jin[l], Shu-Feng Li[a,b], Shui-Qing Liang[m], Jia Liu[a,b], Xiao-Yan Liu[n], Sarah Sherlock[d], Teresa Spicer[a], Gaurav Srivastava[o], He Tang[a,c], Paul Valdes[g], Teng-Xiang Wang[a,c], Mike Widdowson[p], Meng-Xiao Wu[a,c], Yao-Wu Xing[a,b], Cong-Li Xu[a], Jian Yang[q], Cong Zhang[r], Shi-Tao Zhang[s], Xin-Wen Zhang[a,c], Fan Zhao[a], and Zhe-Kun Zhou[a,b,j,1]

[a]CAS Key Laboratory of Tropical Forest Ecology, Xishuangbanna Tropical Botanical Garden, Chinese Academy of Sciences, Mengla 666303, China; [b]Center of Plant Ecology, Core Botanical Gardens, Chinese Academy of Sciences, Mengla 666303, China; [c]University of Chinese Academy of Sciences, 100049 Beijing, China; [d]School of Environment, Earth and Ecosystem Sciences, The Open University, Milton Keynes, MK7 6AA, United Kingdom; [e]Key Laboratory of Vertebrate Evolution and Human Origins, Institute of Vertebrate Paleontology and Paleoanthropology, Chinese Academy of Sciences, 100044 Beijing, China; [f]Center for Excellence in Life and Paleoenvironment, Chinese Academy of Sciences, 100101 Beijing, China; [g]School of Geographical Sciences and Cabot Institute, University of Bristol, Bristol, BS8 1TH, United Kingdom; [h]CAS Center for Excellence in Tibetan Plateau Earth Sciences, Chinese Academy of Sciences, 100101 Beijing, China; [i]Key Laboratory of Continental Collision and Plateau Uplift, Institute of Tibetan Plateau Research, Chinese Academy of Sciences, 100101 Beijing, China; [j]Key Laboratory for Plant Diversity and Biogeography of East Asia, Kunming Institute of Botany, Chinese Academy of Sciences, 650204 Kunming, China; [k]Center for Integrative Conservation, Xishuangbanna Tropical Botanical Garden, Chinese Academy of Sciences, Mengla 666303, China; [l]State Key Laboratory of Biocontrol and Guangdong Key Laboratory of Plant Resources, School of Life Sciences, Sun Yat-sen University, Guangzhou 510275, China; [m]Public Technology Service Center, Xishuangbanna Tropical Botanical Garden, Chinese Academy of Sciences, Mengla 666303, China; [n]School of Geography, South China Normal University, 510631 Guangzhou, China; [o]Cenozoic Palaeofloristic Megafossil Lab, Birbal Sahni Institute of Paleosciences, Lucknow 226 007, India; [p]School of Environmental Sciences, University of Hull, Hull HU6 7RX, United Kingdom; [q]State Key Laboratory of Systematic and Evolutionary Botany, Institute of Botany, Chinese Academy of Sciences, Beijing 100093, China; [r]State Key Laboratory of Continental Tectonics and Dynamics, Institute of Geology, Chinese Academy of Geological Sciences, 100037 Beijing, China; and [s]Faculty of Land Resource Engineering, Kunming University of Science and Technology, 650093 Kunming, China

Tibet's ancient topography and its role in climatic and biotic evolution remain speculative due to a paucity of quantitative surface-height measurements through time and space, and sparse fossil records. However, newly discovered fossils from a present elevation of ~4,850 m in central Tibet improve substantially our knowledge of the ancient Tibetan environment. The 70 plant fossil taxa so far recovered include the first occurrences of several modern Asian lineages and represent a Middle Eocene (~47 Mya) humid subtropical ecosystem. The fossils not only record the diverse composition of the ancient Tibetan biota, but also allow us to constrain the Middle Eocene land surface height in central Tibet to ~1,500 ± 900 m, and quantify the prevailing thermal and hydrological regime. This "Shangri-La"–like ecosystem experienced monsoon seasonality with a mean annual temperature of ~19 °C, and frosts were rare. It contained few Gondwanan taxa, yet was compositionally similar to contemporaneous floras in both North America and Europe. Our discovery quantifies a key part of Tibetan Paleogene topography and climate, and highlights the importance of Tibet in regard to the origin of modern Asian plant species and the evolution of global biodiversity.

biodiversity | fossil | monsoon | Tibetan Plateau | topography

The Tibetan Plateau, once thought of as entirely the product of the India–Eurasia collision, is known to have had significant complex relief before the arrival of India early in the Paleogene (1–3). This large region, spanning ~2.5 million km^2, is an amalgam of tectonic terranes that impacted Asia long before India's arrival (4, 5), with each accretion contributing orographic heterogeneity that likely impacted climate in complex ways. During the Paleogene, the Tibetan landscape comprised a high (>4 km) Gangdese mountain range along the southern margin of the Lhasa terrane (2), against which the Himalaya would later rise (6), and a Tanghula upland on the more northerly Qiangtang terrane (7). Separating the Lhasa and Qiangtang blocks is the east–west trending Banggong-Nujiang Suture (BNS), which today hosts several sedimentary basins (e.g., Bangor, Nyima, and Lunpola) where >4 km of Cenozoic sediments have accumulated (8). Although these sediments record the climatic and biotic evolution of central Tibet, their remoteness means fossil collections

have been hitherto limited. Recently, we discovered a highly diverse fossil assemblage in the Bangor Basin. These fossils characterize a luxuriant seasonally wet and warm Shangri-La forest that once occupied a deep central Tibetan valley along the BNS, and provide a unique opportunity for understanding the evolutionary history of Asian biodiversity, as well as for quantifying the paleoenvironment of central Tibet.*

Significance

The ancient topography of the Tibetan Plateau and its role in biotic evolution are still poorly understood, mostly due to a lack of fossil evidence. Our discovery of ~47-Mya plant fossils from a present elevation of 4,850 m in central Tibet, diminishes, significantly, that lack of knowledge. The fossils represent a humid subtropical vegetation and some of the 70 different plant forms show affinity to Early-Middle Eocene floras in both North America and Europe. Using leaf architecture, we calculate that the forest grew at ~1,500-m elevation within an east–west trending valley under a monsoonal climate. Our findings highlight the complexity of Tibet's ancient landscape and emphasize the importance of Tibet in the history of global biodiversity.

EARTH, ATMOSPHERIC, AND PLANETARY SCIENCES

ECOLOGY

Details of the topographic evolution of Tibet are still unclear despite decades of investigation (4, 5). Isotopic compositions of carbonates recovered from sediments in some parts of central Tibet have been interpreted in terms of high (>4 km) Paleogene elevations and aridity (9, 10), but those same successions have yielded isolated mammal (11), fish (12), plant (13–18), and biomarker remains (19) more indicative of a low (≤3-km) humid environment, but how low is poorly quantified. Given the complex assembly of Tibet, it is difficult to explain how a plateau might have formed so early and then remained as a surface of low relief during subsequent compression from India (20). Recent evidence from a climate model-mediated interpretation of palm fossils constrains the BNS elevation to below 2.3 km in the Late Paleogene (16), but more precise paleoelevation estimates are required. Further fossil discoveries, especially from earlier in the BNS sedimentary records, would document better the evolution of the Tibetan biota, as well as informing our understanding of the elevation and climate in an area that now occupies the center of the Tibetan Plateau.

Our work shows that the BNS hosted a diverse subtropical ecosystem at ~47 Ma, and this means the area must have been both low and humid. The diversity of the fossil flora allows us to 1) document floristic links to other parts of the Northern Hemisphere, 2) characterize the prevailing paleoclimate, and 3) quantify the elevation at which the vegetation grew. We propose that the "high and dry" central Tibet inferred from some isotope paleoaltimetry (9, 10) reflects a "phantom" elevated paleosurface (20) because fractionation over the bounding mountains allowed only isotopically light moist air to enter the valley, giving a false indication of a high elevation (21).

Results and Discussion

Species Diversity in the Middle Eocene of Central Tibet. The Jianglang biota (31.625121°N, 90.029038°E, 4,850 m above mean sea level (a.m.s.l.), Fig. 1 and *SI Appendix*, Fig. S1) occurs in five outcrops all within 1.5 km of each other in the Bangor Basin, central Tibetan Plateau. Each outcrop represents a different horizon within a 26-m succession of lacustrine mudstones (Fig. 1C and *SI Appendix*, Figs. S1 and S2) The entire fossil-bearing section is assigned to the middle part of the Paleocene–Eocene Niubao Formation, and contains a tephra-rich horizon just below fossil assemblage XZBGJL5, dated here as no older than 47.5 ± 0.7 Ma based on the U-Pb age of the youngest zircon population (bed 9 in Fig. 1C and *SI Appendix*, Table S1) The Niubao Formation underlies the palm-bearing (16) Dingqing Formation, the lower part of which is dated as 23.5 ± 0.2 Ma (22) and the middle to upper parts as 20.7 ± 0.1 Ma (23), also based on zircon U-Pb ages of lacustrine tephras. A Late Paleogene biota from the lower part of the Dingqing Formation yields plants (13, 15–18), insects (24), mammals (11), and fishes (12), all indicative of warm and humid conditions at low elevation (16).
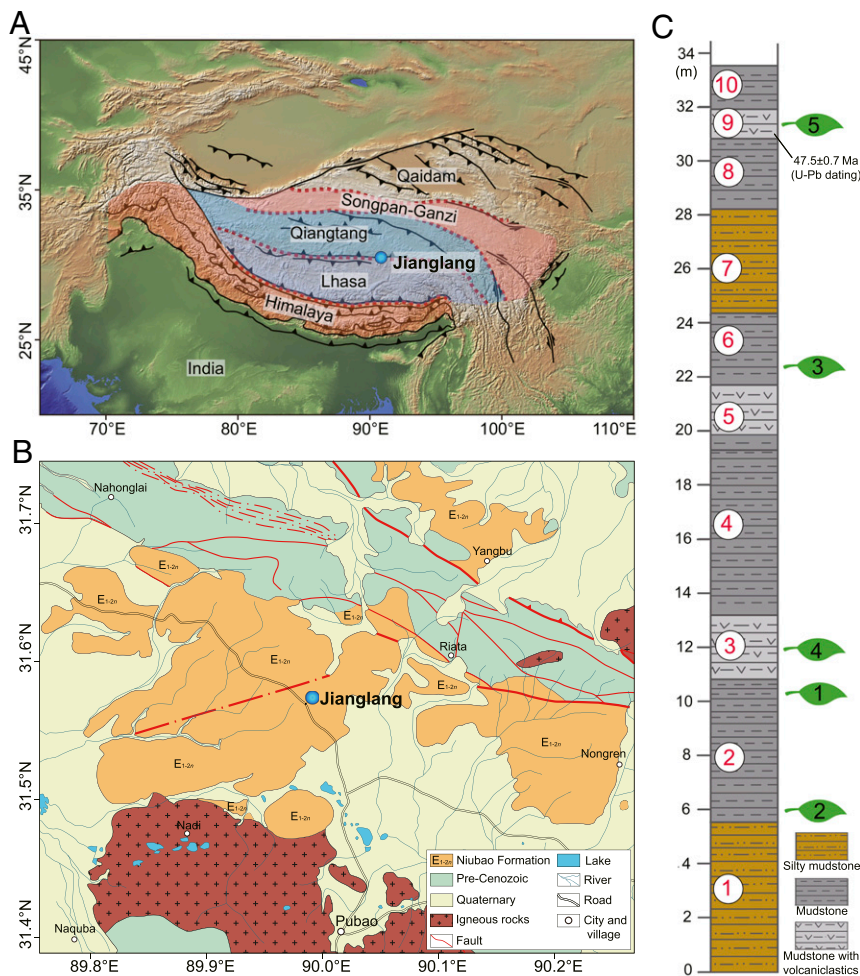

Fig. 1. Map showing the fossil site near Jianglang village, Bangor Basin, central Tibet. (A) Location in relation to major terranes of the Tibetan Plateau. (B) Geological map showing the fossil site and adjacent area. (C) Stratigraphy of the Niubao Formation in the fossil site, Bangor Basin. Assemblage numbers indicated by leaf icons, bed numbers in red.

The Jianglang flora comprises 70 plant fossil morphotypes in various states of preservation (*SI Appendix*, Fig. S3*A*). Numerous leaf, fruit, seed, flower, branch, and tuber (Fig. 2 and *SI Appendix*, Figs. S4–S8 and Table S2) remains make it the richest Cenozoic flora on the plateau so far discovered. Among these fossils, leaves are the most abundant with 42 distinct morphotypes (broadly equivalent to species), followed by 24 fruit/seed types (*SI Appendix*, Table S2). None of the modern living relatives of these taxa exist in central Tibet today, and most represent their first fossil records from the plateau, e.g., Apocynaceae, *Ceratophyllum*, *Illigera*, *Lagokarpos*, and Vitaceae (Fig. 2 and *SI Appendix*, Figs. S4–S8). While unique for Tibet in terms of overall assemblage composition, some Jianglang taxa occur in the younger (Late Oligocene) Dayu flora of the Dingqing Formation in the nearby Lunpola Basin. These include *Ailanthus* (13), *Cedrelospermum* (15), *Koelreuteria* (17), and *Limnobiophyllum* (18),

indicating that some genera persisted in the core area of what is now the Tibetan Plateau for perhaps as long as ~25 My. Moreover, fossil insects, fishes, and bird feathers have also been collected from the Jianglang floral layers (*SI Appendix*, Figs. S9 and S10).

Tibet's Role for Global Biodiversity. The contribution of Tibet to global biodiversity in deep time has hitherto been overlooked due to a lack of fossil evidence. The Paleocene and early Eocene "redbeds" of the lower Niubao Formation indicate aridity, but the richness of plant species in the Jianglang flora evidences a diverse subtropical Shangri-La–like valley ecosystem along the BNS. This persisted in a modified form into the late Oligocene as shown by the Lunpola Basin biota (11–13, 15–18, 24). Significantly, these new floral discoveries show that central Tibet hosted a different plant diversity in deep time from that which exists

Fig. 2. Representative plant taxa in the Middle Eocene Jianglang flora from central Tibetan Plateau. (*A*) *Lagokarpos tibetensis* fruit (XZBGJL1-0383). (*B* and *C*) legume fruits (XZBGJL1-0012, XZBGJL3-0009). (*D*) *Koelreuteria* (Sapindaceae) capsular valves (XZBGJL5-0029). (*E*) *Ceratophyllum* (Ceratophyllaceae) achene (XZBGJL5-0545). (*F*) *Stephania* (Menispermaceae) endocarp (XZBGJL5-0524). (*G*) Unknown flower (XZBGJL1-0008). (*H*) cf *Colocasia* (Araceae) tubers (XZBGJL5-0231). (*I*) *Illigera* (Hernandiaceae) fruit (XZBGJL1-0003). (*J*) legume leaflet (XZBGJL5-0123). (*K*) Vitaceae seed (XZBGJL1-0018). (*L*) *Asclepiadospermum marginatum* (Apocynaceae) seed (XZBGJL5-0432). (*M*) Cedreleae (Meliaceae) seed (XZBGJL5-0034). (*N*) *Limnobiophyllum* (Araceae) whole plant (XZBGJL5-0177). (*O*) *Ailanthus maximus* (Simaroubaceae) samara (XZBGJL5-0007). (*P*) *Cedrelospermum* (Ulmaceae) young fruit-bearing branch (XZBGJL5-0033). (*Q*) *Cedrelospermum* (Ulmaceae) leaf (XZBGJL5-0533). (*R*) Myrtales leaf (XZBGJL5-0166). (*S*) *Ziziphus* (Rhamnaceae) leaf (XZBGJL1-0023). (Scale bars, 10 mm: *A, C, D, H, N, O, R, S*; 5 mm: *B, G, I, J, P, Q*; 2 mm: *E, F, K–M*.)

on the plateau now, but many fossil taxa in these Tibetan Paleogene floras still survive at low elevations in regions adjacent to the plateau, e.g., the southern slope of the Himalaya, the Hengduan Mountains, and Southeast Asia, all of which are modern globally significant centers of high biodiversity (25). The numerous first occurrences of taxa within a Middle Eocene central Tibetan lowland surrounded by high relief, and exposed to a temporally varying global climate (26), provide evidence of an ideal setting for biodiversity generation (27), from which lineages dispersed more widely. Because all taxa in the BNS floras no longer exist on the plateau, molecular data alone cannot record the biogeographic history of Tibet. Thus, the Jianglang fossils record the presence and composition of a diverse, but extinct, Tibetan ecosystem that could not be evidenced any other way.

The discovery of the Jianglang biota points to Tibet being a hitherto unrecognized ancient locus of floral diversity. Although the correlation between topographic complexity and biodiversity is well-documented, the relationship between the Tibetan region orography, Asian monsoons, and biodiversity is complex and poorly understood (28). Many components of the Jianglang flora represent the oldest fossil records of those taxa in Asia, e.g., Apocynaceae, *Cedrelospermum*, *Lagokarpos*, and *Limnobiophyllum*, altering our understanding of the early evolution of those plants. Overall, the Jianglang species assemblage is most similar to that of the Early-Middle Eocene Green River flora in the western interior United States of America (USA) (*SI Appendix*, Fig. S11 and Table S2) with ~16 taxa in common at the genus/family level, including some with unclear taxonomic affinities to modern plants (*SI Appendix*, Fig. S11 and Table S2). The Jianglang flora also contains eight taxa in common at the genus/family level with the Middle Eocene Messel flora in Germany (*SI Appendix*, Table S2). The partial taxonomic congruence between the Jianglang flora and contemporaneous plant fossil assemblages in North America and Europe argues for relatively free exchange of lineages across the Northern Hemisphere. Equator-to-pole temperature gradients were remarkably shallow during the Eocene (29), with low-latitude mean annual temperatures being surprisingly cool (<30 °C) for a global "hothouse" (30, 31), and warm polar temperatures (ref. 32 and references therein). This shallow thermal gradient allowed much wider distribution of subtropical and tropical plants into the higher latitudes. Notably, however, taxon exchange between central Tibet and the Indian Plate was limited prior to the Middle Eocene according to current paleobotanical records, with so far only *Ailanthus* demonstrably originating from Gondwana (13). The high (>4-km) Gangdese mountain range along the southern margin of Tibet (2) seems to have provided a significant barrier to plant migration from the south at this time.

Middle Eocene Paleoclimate and Paleoelevation of Central Tibet. The composition of the Jianglang flora demonstrates that a heterogeneous humid subtropical lowland forest existed in central Tibet (*SI Appendix*, Table S2) in the Middle Eocene, and seemingly no single species dominated (*SI Appendix*, Fig. S3A). By reconstructing ancient climate parameters encoded in leaf morphological traits using the Climate-Leaf Analysis Multivariate Program (CLAMP) (http://clamp.ibcas.ac.cn) (33–35) (Datasets S1–S3), we are able to quantify both the climate and elevation of central Tibet in the Middle Eocene.

CLAMP has been applied widely to fossil floras globally (36), and to Cenozoic floras in the Tibetan region (6, 37). This method constructs a 31-dimensional model of leaf trait space using modern vegetation for which the climate is known, and positions fossil floras passively within that space based on their preserved traits. Fig. 3 *A* and *B* show the Jianglang fossil leaf traits are most similar to those seen in modern vegetation adapted to Asian

monsoon climates, from which we infer that the Jianglang paleoclimate was monsoonal.

To position the climate trends (vectors) through trait space we used multiple linear regressions (38) of the climate recorded at the modern vegetation sites. The position of the Jianglang flora within trait space defines its relative position (vector score) along the different vectors. Using vectors positioned within the first four dimensions, which capture 70% of the total variation, a second-order polynomial regression between the vector score and observations translates the vector score of the fossil flora into the predicted paleoclimate. Fig. 3 *C* and *D* show regressions for mean annual temperature (MAT) and moist enthalpy. Regressions for all other climate parameters returned by CLAMP are given in *SI Appendix*, Figs. S12–S15.

The Jianglang leaf traits indicate a mean annual air temperature of 19 ± 2.4 °C, a cold-month mean temperature of 7 ± 2.9 °C (and so mostly frost-free), and a maximum temperature of the coldest month of 14 ± 3.5 °C. The growing season lasted 11 ± 1 mo. Rainfall during those 11 mo was high at ~2 m, but precipitation was markedly seasonal (wet season: dry season ratio of ~6:1) consistent with a model-predicted valley system (16) and a regional monsoon (40), although the dry season (winter) was short. Despite low rainfall, winter coolness produced the highest humidity with a December–February vapor pressure deficit of 5.6 ± 1.5 hPa as against a summer (June–August) value of 14.8 ± 3.5 hPa, when temperatures in the warmest month averaged ≥28 °C and rarely fell below 22 ± 2.9 °C. All of the Jianglang climate estimates, with uncertainties, are given in *SI Appendix*, Table S3.

The subtropical nature of the flora, even at a Middle Eocene latitude possibly ~9° further south (41, 42), implies a relatively low paleoelevation. We calculate the elevation of the lake margin forest using moist enthalpy, also derived from Jianglang leaf form, and use model mediation to obtain a Jianglang sea-level datum (*Materials and Methods*) (Fig. 3D). This approach yields a paleoelevation of 1.5 ± 0.9 km for the Jianglang vegetation, so below the 2.3-km upper bound indicated by the Late Paleogene palms, and above the inferred ~1-km surface height of the northern Lhasa terrane at 55 Ma (43). This result is also in agreement with a low "near sea-level" Late Eocene (~39 Ma) elevation for the Gerze Basin further west along the BNS (44).

Our results show that central Tibet in the Middle Eocene was neither high nor dry (9, 10), but low and humid (*SI Appendix*, Fig. S16). The discrepancy with isotope-derived paleoelevation estimates can be explained in terms of the rain-out removal of heavy isotopes as predominantly northward monsoon summer airflows passed over the Gangdese mountains, and dry, isotopically light air from the Asian interior flowed southward over the Tanghula highlands in winter. The resulting isotopically light hydrological system in the central valley, with model moisture pathways suggesting little opportunity for east or west airmass $\delta^{18}O$ enrichment (20), therefore reflects the height of the bounding mountain crests, and so appears as a phantom high plateau (21).

In extremis, it could be argued that the apparently subtropical Eocene flora represents an extinct biota specially adapted to high and dry conditions, and not a valley system at all. But if this were the case, we would have to invoke, across many taxa, unique highly advantageous biological adaptations that no longer exist. This is a form of special pleading that seems implausible because suitable environments favoring such adaptations became more widespread during progressive Cenozoic cooling, meaning that if such biological adaptations ever did exist, they should be widespread today, which they are not. Furthermore, modeling experiments show that simply having a plateau, even one as low as 2.5 km, will induce significant drying across its surface (*SI Appendix*, Fig. S17).

The subtropical central lowland did not persist long into the Neogene (*SI Appendix*, Fig. S16). The disappearance of the Jianglang biota and the formation of a plateau-like elevated surface, but
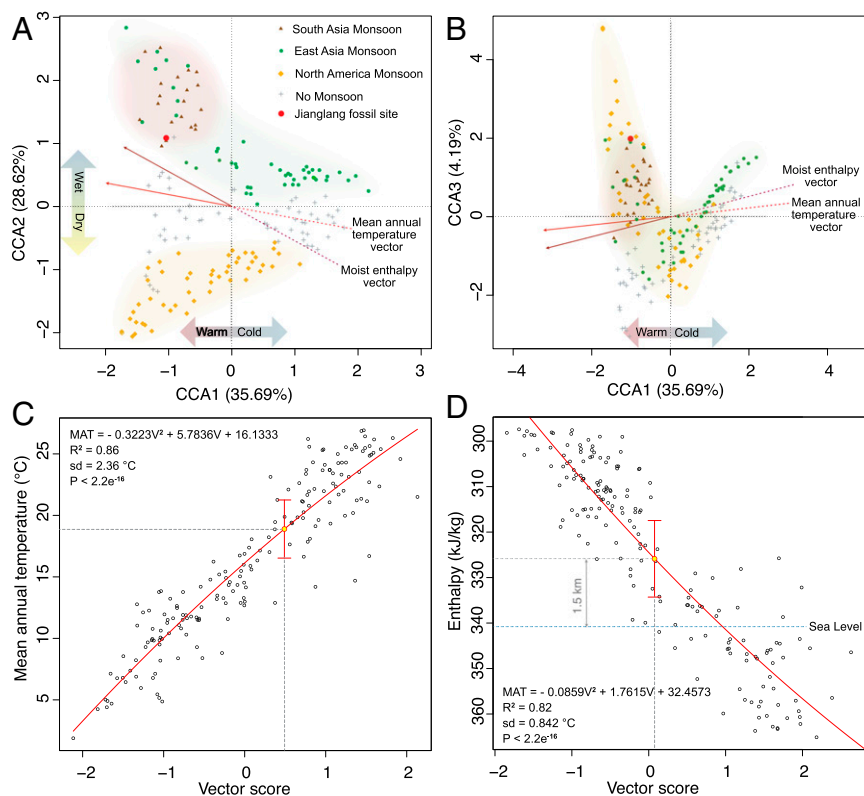
Fig. 3. CLAMP physiognomic space plots showing the positions of modern vegetation reference sites coded for their adaptations to different monsoon climates (39). (*A*) CCA axis 1 (accounting for 35.69% of the total variance) versus axis 2 (28.62%). The Jianglang site (filled red circle) plots near modern vegetation exhibiting adaptations to both the South Asian (Indian) monsoon and the East Asia monsoon. (*B*) CCA axis 1 versus axis 3 (4.19%) showing the clear separation of the Jianglang fossil site from nonmonsoon adapted vegetation. The apparent proximity to the North American monsoon sites is an artifact of the projection. The climate trends across physiognomic space are shown for mean annual temperature (red arrow) and moist enthalpy (purple arrow). (*C*) MAT regression. The vector score is the relative position along the MAT vector in axes 1–4 space of the modern vegetation samples (open black circles) for which the MAT is known, and the fossil site (yellow-filled circle). The estimate of the MAT for the fossil site is given by its vector score (V), which defines its position along the regression curve and hence the MAT estimate. Two sigma uncertainties are indicated by the red bars. (*D*) The moist enthalpy regression showing both the position of the Jianglang fossil site and sea-level moist enthalpy derived from a climate model simulation constrained by proxy data (see *Materials and Methods* for details). The difference in moist enthalpy between sea level and the Jianglang site (14.75 kJ/kg) divided by the gravitational constant (9.81 cm/s^2) yields an elevational difference of 1.5 km.

with more relief than now, was likely caused by 1) the rise of the BNS valley floor by northward compression and sediment infilling of the semi-enclosed bathtub-like valley system (16), 2) Neogene drying resulting from the retreat of the Neotethys Ocean (45), as well as 3) the rise of the Himalaya during the Miocene (6, 46), which further hindered moisture penetration into the Tibetan interior from the Indian Ocean. Thus, a high landscape approximating the present plateau formed in the Neogene (*SI Appendix*, Fig. S16), not solely through a process of tectonic "uplift" with Tibet behaving as a coherent entity, but by a process of gradual evolution of compression-driven landscape modification and "bathtub sedimentation" (47).† These complex landscape changes would have provided a heterogeneous environmental niche matrix within which numerous speciation events would have taken place (48). In the future, the ancient complexity of Tibetan topography needs to be considered when studying the evolution of the modern plateau and its influence on climate and biodiversity (20).

Conclusions

The Jianglang flora provides solid evidence for high plant diversity in central Tibet during the Middle Eocene (~47 Ma). Some genera survived there for at least ~25 My, as shown by

their persistence into the Late Oligocene Dayu flora from the Dingqing Formation within the Lunpola Basin (13, 15, 17, 18). Many taxa in the Jianglang flora, e.g., Apocynaceae, *Ceratophyllum*, *Illigera*, *Lagokarpos*, and Vitaceae, represent new discoveries for the plateau, and some are the oldest fossil records for these taxa in Asia, e.g., Apocynaceae, *Cedrelospermum*, *Lagokarpos*, and *Limnobiophyllum*. The floristic composition of the Jianglang flora is remarkably similar to other Early-Middle Eocene floras in the Northern Hemisphere, such as the Green River flora in western interior USA and the Messel flora in Germany. However, the Jianglang flora shows little affinity to Eocene floras from Indian Plate; only *Ailanthus* demonstrably originated from Gondwana. Since many genera in the Jianglang flora still survive in regions adjacent to the Tibetan Plateau, the discovery of this flora demonstrates the importance of the central Tibetan region to species origins and evolution in Asia, as well as having a role in floristic exchange within the Northern Hemisphere. Such a role would be impossible to infer from molecular data alone.

The composition of the Jianglang flora evidences a diverse Middle Eocene subtropical lowland forest in central Tibet, adapted to a monsoonal climate at ~1,500-m elevation within an east–west trending valley. This valley, and the ecosystem it hosted, persisted until the Miocene, when the high elevation of today's central Tibetan Plateau was formed by northward compression and sediment infilling of topographic lows. In the future, the

---

†Uplift here refers exclusively to work done against gravity (56).

complex topography of Tibet in the geological past needs to be considered when studying the paleoenvironmental and biodiversity histories on the plateau.

Materials and Methods

Geological Setting. The fossil site is located near Jianglang village, about 25 km north of Pubao Town, Bangor County, central Tibetan Plateau. The fossil-bearing horizons belong to the widely distributed ~3,000-m-thick Niubao Formation, which has been assigned a Paleocene-Eocene age (49). While the Niubao Formation mostly consists of red sandstones, the fossils described here are preserved in gray mudstones in the middle part of the formation.

Zircons were handpicked from crushed samples of a tephra-rich horizon just below the fossil assemblage XZBGJL5 (Fig. 1 and *SI Appendix*, Fig. S2). They were mounted in epoxy resin and polished down to expose grain centers. Representative zircons for analysis were selected by both micrograph and cathodoluminescence imaging, which was conducted with an FEI Nova 450 Nano Scanning Electron Microscope. U-Pb dating was performed using both a Neptune Laser Ablation Multicollector Inductively Coupled Plasma Mass Spectrometer (LA-MC-ICP-MS) at the Institute of Geology, Chinese Academy of Geological Sciences, and a Thermo Fisher iCAP Qnova Laser Ablation Inductively Coupled Plasma Mass Spectrometer (LA-ICP-MS) at Peking University. The isotope data were collected in sets of five scans with a reference zircon 91500 sample (1,062 Ma) and processed by ICPMS DataCal 8.4 software. Ninety-five analysis points on 95 zircons yielded $^{206}Pb/^{238}U$ ages between 2,513.0 ± 33.0 Ma and 46.7 ± 1.1 Ma (*SI Appendix*, Table S1). Eighteen analyses defined an age peak at ~117.6 Ma in the relative probability diagram, which represents the age of the main material source (*SI Appendix*, Table S1). The youngest zircons with a Concordia age of 47.5 ± 0.7 Ma show the oldest depositional age of the rock. This age accords with the floral similarities to Eocene assemblages in the western USA (Green River) and Germany (Messel), and indicates the age of this flora to be the Middle Eocene, but no older than ~47 Ma.

Fossil Identification and Floristic Comparison. Fossils were collected from five layers, each layer assigned a different number (Fig. 1 and *SI Appendix*, Fig. S1). Incident light imaging employed a digital camera (Nikon D700) and morphological detail was observed using a stereo microscope (Leica S8APO). Plant fossils were compared to modern and fossil taxa imaged in online data sources, including the Chinese Virtual Herbarium (https://www.cvh.ac.cn/), the Herbarium of Kew Royal Botanic Gardens (http://apps.kew.org), and the Cenozoic Angiosperm Database (CAD, http://www.fossil-cad.net/). All plant fossils are deposited in the Paleoecology Collections, Xishuangbanna Tropical Botanical Garden (XTBG), Chinese Academy of Sciences (CAS). Rarefaction, utilizing packages of iNext (V. 2.0.20) and ggplot2 (V 3.3.1) in R software (V 4.0.0), was used to estimate species richness of the Jianglang flora (*SI Appendix*, Fig. S3B).

Paleoclimate Reconstruction. To reconstruct the paleoclimate quantitatively we employed CLAMP (http://clamp.ibcas.ac.cn), which is used widely for paleoclimate reconstruction (36). Leaf layer 5 (XZBGJL5) yielded 31 fossil morphotypes satisfying the CLAMP minimum diversity requirement of 20, and scored (Dataset S1) using standard CLAMP protocols. Inevitably not all leaf fossils are complete, so CLAMP incorporates a completeness metric that varies between 0 (no leaves preserved) and 1 (all leaves complete). Completeness scores less than 0.6 increase the uncertainty (http://clamp.ibcas.ac.cn). The Jianglang flora has a score >0.8 (Dataset S1).

The PhysgAsia2 physiognomic file (50) (Dataset S2), paired with a new 1-km resolution gridded climate dataset, WorldClim2 (51) (Dataset S3), was used to calibrate CLAMP. This calibration yields a wider range of climate variables than previous CLAMP analyses, but otherwise gives similar results. The calibration data, full analytical results (*SI Appendix*, Table S3), and CLAMP regression models (*SI Appendix*, Figs. S12–S15) are given as *SI Appendix*.

Paleoelevation Reconstruction. Paleoelevation reconstruction employed the difference in moist enthalpy derived from the CLAMP analysis, and a moist enthalpy prediction at sea level for the Jianglang site as derived from the HadCM3L climate model; a coupled Atmosphere Ocean General Circulation model, with a resolution of 3.75° × 2.5° longitude × latitude in the atmosphere and ocean (specifically HadCM3BL-M2.1aD) (52). CO_2 was set to 1,120 ppm (53) with a solar constant calculated for the Lutetian (54) making use of already fully equilibrated (10,422 model years) sea-surface temperature and salinity fields from a previously spun-up version of the Lutetian (55). The model simulation used a Lutetian paleogeography supplied by Getech Plc., modified to accommodate a Tibet with a central valley where the valley floor was 2 km a.m.s.l. and the Jianglang site was at a paleolatitude at 22.5°N. The model was run for 200 y with the moist enthalpy means produced from the last 100 y of the simulation. The same model was used to explore the effect on precipitation of configuring the paleotopography for a plateau at different elevations (*SI Appendix*, Fig. S17).

Model and proxy data are rarely directly comparable, and this raw model result had to be adjusted to be compatible with the CLAMP proxy. There is no contemporaneous sea-level fossil site adjacent to the Jianglang flora and moist enthalpy varies zonally, so to obtain a CLAMP datum at the Jianglang site, we used a latitudinal spread of 7 Early to Middle Eocene sea-level sites in the CLAMP archive (clamp.ibcas.ac.cn) from paleolatitude 5.53 °N (Gurha, N.W. India) to 73.25°N (Svalbard). Because the difference between the model latitudinal moist enthalpy gradient and that yielded by CLAMP varies with latitude, we used the empirically obtained CLAMP/model latitudinal difference gradient ($y = -0.7167x + 14.4466$) (x is paleolatitude, y is adjusted moist enthalpy at sea level; *SI Appendix*, Table S4) to adjust the Jianglang raw model enthalpy value at sea level (338.99 kJ/kg) by 1.66 kJ/kg to obtain 340.65 kJ/kg, a value compatible with that obtained by CLAMP from the fossil flora at the paleosurface.

Using the equation of Forest et al. (34),

$$Z = (H_{low} - H_{high})/g,$$

where H_{low} is the adjusted-to-CLAMP model-derived moist enthalpy at sea level, H_{high} is the CLAMP-derived moist enthalpy from the Jiangliang flora, and g is the acceleration due to gravity (a constant with the value 9.81 cm/s²), we obtained the elevation of the flora (Z) as (340.65−325.9)/9.81 = 1.50 km.

The CLAMP regression uncertainty combined with that shown by the model/CLAMP differences gave an overall uncertainty of ± 0.9 km (1 SD).

Data Availability. All study data are included in the article and *SI Appendix*.

1. P. England, M. Searle, The Cretaceous-Tertiary deformation of the Lhasa block and its implications for crustal thickening in Tibet. *Tectonics* **5**, 1–14 (1986).
2. L. Ding et al., The Andean-type Gangdese mountains: Paleoelevation record from the Paleocene–Eocene Linzhou basin. *Earth Planet. Sci. Lett.* **392**, 250–264 (2014).
3. S. Guillot et al., How and when did the Tibetan plateau grow? *Russ. Geol. Geophys.* **60**, 957–977 (2019).
4. C.-F. Chang, X.-L. Zheng, Some tectonic features of the Mt. Jolmo Lungma area, southern Tibet. *Sci. Sin.* **16**, 257–265 (1973).
5. P. Kapp, P. G. DeCelles, Mesozoic-Cenozoic geological evolution of the Himalayan-Tibetan orogen and working tectonic hypotheses. *Am. J. Sci.* **319**, 159–254 (2019).
6. L. Ding et al., Quantifying the rise of the Himalaya orogen and implications for the South Asian monsoon. *Geology* **45**, 215–218 (2017).
7. Q. Xu et al., Paleogene high elevations in the Qiangtang terrane, central Tibetan plateau. *Earth Planet. Sci. Lett.* **362**, 31–42 (2013).
8. J. Wang et al., *The Potential of the Oil and Gas Resources in Major Sedimentary Basins on the Qinghai-Xizang, (Tibet) Plateau* (Geological Publishing House, Beijing, 2004).
9. P. G. DeCelles et al., High and dry in central Tibet during the late Oligocene. *Earth Planet. Sci. Lett.* **253**, 389–401 (2007).
10. D. B. Rowley, B. S. Currie, Palaeo-altimetry of the late Eocene to Miocene Lunpola Basin, central Tibet. *Nature* **439**, 677–681 (2006).

11. T. Deng *et al.*, A mammalian fossil from the Dingqing Formation in the Lunpola Basin, northern Tibet, and its relevance to age and paleo-altimetry. *Chin. Sci. Bull.* **57**, 261–269 (2012).

12. F. Wu, D. Miao, M. M. Chang, G. Shi, N. Wang, Fossil climbing perch and associated plant megafossils indicate a warm and wet central Tibet during the late Oligocene. *Sci. Rep.* **7**, 878 (2017).

13. J. Liu *et al.*, Biotic interchange through lowlands of Tibetan Plateau suture zones during Paleogene. *Palaeogeogr. Palaeoclimatol. Palaeoecol.* **524**, 33–40 (2019).

14. H. Tang *et al.*, Extinct genus *Lagokarpos* reveals a biogeographic connection between Tibet and other regions in the Northern Hemisphere during the Paleogene. *J. Syst. Evol.* **57**, 670–677 (2019).

15. L.-B. Jia *et al.*, First fossil record of *Cedrelospermum* (Ulmaceae) from the Qinghai-Tibetan Plateau: Implications for morphological evolution and biogeography. *J. Syst. Evol.* **57**, 94–104 (2019).

16. T. Su *et al.*, No high Tibetan Plateau until the Neogene. *Sci. Adv.* **5**, eaav2189 (2019).

17. H. Jiang *et al.*, Oligocene *Koelreuteria* (Sapindaceae) from the Lunpola Basin in central Tibet and its implication for early diversification of the genus. *J. Asian Earth Sci.* **175**, 99–108 (2019).

18. S. L. Low *et al.*, Oligocene *Limnobiophyllum* (Araceae) from the central Tibetan Plateau and its evolutionary and palaeoenvironmental implications. *J. Syst. Palaeontology* **18**, 415–431 (2020).

19. G. D. Jia, Y. Bai, Y. Ma, J. Sun, P. Peng, Paleoelevation of Tibetan Lunpola basin in the Oligocene-Miocene transition estimated from leaf wax lipid dual isotopes. *Global Planet. Change* **126**, 14–22 (2015).

20. R. A. Spicer *et al.*, Why the 'uplift of the Tibetan Plateau' is a myth. *Natl. Sci. Rev.*, 10.1093/nsr/nwaa091 (2020).

21. L. H. Deng, G. D. Jia, High-relief topography of the Nima basin in central Tibetan Plateau during the mid-Cenozoic time. *Chem. Geol.* **493**, 199–209 (2018).

22. H. Y. He, J. M. Sun, Q. L. Li, R. X. Zhu, New age determination of the Cenozoic Lunpola basin, central Tibet. *Geol. Mag.* **149**, 141–145 (2012).

23. Z.-Q. Mao *et al.*, Recognition of tuffs in the middle-upper Dingqinghu Fm., Lunpola Basin, central Tibetan Plateau: Constraints on stratigraphic age and implications for paleoclimate. *Palaeogeogr. Palaeoclimatol. Palaeoecol.* **525**, 44–56 (2019).

24. C. Y. Cai, D. Y. Huang, F. X. Wu, M. Zhao, N. Wang, Tertiary water striders (Hemiptera, Gerromorpha, Gerridae) from the central Tibetan Plateau and their palaeobiogeographic implications. *J. Asian Earth Sci.* **175**, 121–127 (2019).

25. N. Myers, R. A. Mittermeier, C. G. Mittermeier, G. A. B. da Fonseca, J. Kent, Biodiversity hotspots for conservation priorities. *Nature* **403**, 853–858 (2000).

26. E. Anagnostou *et al.*, Changing atmospheric CO_2 concentration was the primary driver of early Cenozoic climate. *Nature* **533**, 380–384 (2016).

27. C. Rahbek *et al.*, Building mountain biodiversity: Geological and evolutionary processes. *Science* **365**, 1114–1119 (2019).

28. R. A. Spicer, Tibet, the Himalaya, Asian monsoons and biodiversity–In what ways are they related? *Plant Divers.* **39**, 233–244 (2017).

29. D. R. Greenwood, S. L. Wing, Eocene continental climates and latitudinal temperature gradients. *Geology* **23**, 1044–1048 (1995).

30. R. A. Spicer *et al.*, Cool tropics in the middle Eocene: Evidence from the Changchang flora, Hainan Island, China. *Palaeogeogr. Palaeoclimatol. Palaeoecol.* **412**, 1–16 (2014).

31. C. R. Keating-Bitonti, L. C. Ivany, H. P. Affek, P. Douglas, S. D. Samson, Warm, not super-hot, temperatures in the early Eocene subtropics. *Geology* **39**, 771–774 (2011).

32. M. Salpin *et al.*, Evidence for subtropical warmth in the Canadian Arctic (Beaufort-Mackenzie, Northwest territories, Canada) during the early Eocene. *Spec. Pap. Geol. Soc. Am.* **541**, 637–664 (2019).

33. J. Yang, R. A. Spicer, T. E. V. Spicer, C.-S. Li, 'CLAMP online': A new web-based palaeoclimate tool and its application to the terrestrial Paleogene and Neogene of North America. *Palaeobiodivers. Palaeoenviron.* **91**, 163–183 (2011).

34. C. E. Forest, P. Molnar, K. A. Emanuel, Palaeoaltimetry from energy conservation principles. *Nature* **374**, 347–350 (1995).

35. C. E. Forest, J. A. Wolfe, P. Molnar, K. A. Emanuel, Palaeoaltimetry incorporating atmospheric physics and botanical estimates of palaeoclimate. *Geol. Soc. Am. Bull.* **111**, 497–511 (1999).

36. J. Yang *et al.*, Leaf form-climate relationships on the global stage: An ensemble of characters. *Glob. Ecol. Biogeogr.* **24**, 1113–1125 (2015).

37. B. W. Song *et al.*, Qaidam Basin leaf fossils show northeastern Tibet was high, wet and cool in the early Oligocene. *Earth Planet. Sci. Lett.* **537**, 116175 (2020).

38. C. J. F. ter Braak, The analysis of vegetation-environment relationships by canonical correspondence analysis. *Vegetatio* **69**, 69–77 (1987).

39. R. A. Spicer *et al.*, Asian Eocene monsoons as revealed by leaf architectural signatures. *Earth Planet. Sci. Lett.* **449**, 61–68 (2016).

40. A. Farnsworth *et al.*, Past East Asian monsoon evolution controlled by paleogeography, not CO2. *Sci. Adv.* **5**, eaax1697 (2019).

41. W. T. Huang *et al.*, What was the Paleogene latitude of the Lhasa terrane? A reassessment of the geochronology and paleomagnetism of Linzizong volcanic rocks (Linzhou basin, Tibet). *Tectonics* **34**, 594–622 (2015).

42. P. C. Lippert, X. Zhao, R. S. Coe, C.-H. Lo, Palaeomagnetism and $^{40}Ar/^{39}Ar$ geochronology of upper palaeogene volcanic rocks from central Tibet: Implications for the central Asia inclination anomaly, the palaeolatitude of Tibet and post-50 Ma shortening within Asia. *Geophys. J. Int.* **184**, 131–161 (2011).

43. R. Hetzel *et al.*, Peneplain formation in southern Tibet predates the India-Asia collision and plateau uplift. *Geology* **39**, 983–986 (2011).

44. Y. Wei *et al.*, Low palaeoelevation of the northern Lhasa terrane during late Eocene: Fossil foraminifera and stable isotope evidence from the Gerze Basin. *Sci. Rep.* **6**, 27508 (2016).

45. N. McQuarrie, J. M. Stock, C. Verdel, B. P. Wernicke, Cenozoic evolution of Neotethys and implications for the causes of plate motions. *Geophys. Res. Lett.* **30**, 2036 (2003).

46. A. Gébelin *et al.*, The Miocene elevation of Mount Everest. *Geology* **41**, 799–802 (2013).

47. P. Tapponnier *et al.*, Oblique stepwise rise and growth of the Tibet plateau. *Science* **294**, 1671–1677 (2001).

48. R. A. Spicer, A. Farnsworth, T. Su, Cenozoic topography, monsoons and biodiversity conservation within the Tibetan Region: An evolving story. *Plant Divers.* **42**, 229–254 (2020).

49. S. X. Zhang, *Geological Formation Names of China (1866–2000)* (Higher Education Press, Beijing and Springer-Verlag, Berlin, 2009).

50. M. A. Khan *et al.*, Miocene to pleistocene floras and climate of the eastern Himalayan Siwaliks, and new palaeoelevation estimates for the Namling-Oiyug basin, Tibet. *Global Planet. Change* **113**, 1–10 (2014).

51. S. E. Fick, R. J. Hijmans, WorldClim 2: New 1-km spatial resolution climate surfaces for global land areas. *Int. J. Climatol.* **37**, 4302–4315 (2017).

52. P. J. Valdes *et al.*, The BRIDGE HadCM3 family of climate models: HadCM3@Bristol v1.0. *Geosci. Model Dev.* **10**, 3715–3743 (2017).

53. G. L. Foster, D. L. Royer, D. J. Lunt, Future climate forcing potentially without precedent in the last 420 million years. *Nat. Commun.* **8**, 14845 (2017).

54. D. O. Gough, Solar interior structure and luminosity variations. *Sol. Phys.* **74**, 21–34 (1981).

55. A. Farnsworth *et al.*, Climate sensitivity on geological timescales controlled by non-linear feedbacks and ocean circulation. *Geophys. Res. Lett.* **46**, 9880–9889 (2019).

56. P. Molnar, P. England, Late Cenozoic uplift of mountain ranges and global climate change: Chicken or egg? *Nature* **346**, 29–34 (1990).

EARTH, ATMOSPHERIC, AND PLANETARY SCIENCES

ECOLOGY